

Periodic Flare of the 6.7 GHz Methanol Maser in IRAS 22198+6336

Kenta FUJISAWA,^{1,2} Genta TAKASE,¹ Saki KIMURA,¹ Nozomu AOKI,¹ Yoshito NAGADOMI,¹
Tadashi SHIMOMURA,¹ Koichiro SUGIYAMA,¹ Kazuhito MOTOGI,¹ Kotaro NIINUMA,¹
Tomoya HIROTA,³ and Yoshinori YONEKURA⁴

¹*Department of Physics, Faculty of Science, Yamaguchi University, Yoshida 1677-1, Yamaguchi-city,
Yamaguchi 753-8512*

²*The Research Institute of Time Studies, Yamaguchi University, Yoshida 1677-1, Yamaguchi-city,
Yamaguchi 753-8511*

³*Mizusawa VLBI Observatory, National Astronomical Observatory of Japan, Hoshigaoka-cho 2-12,
Oshu, Iwate 023-0861*

⁴*Center for Astronomy, Ibaraki University, 2-1-1 Bunkyo, Mito, Ibaraki 310-8512*
kenta@yamaguchi-u.ac.jp

(Received ; accepted)

Abstract

We have detected periodic flares of the 6.7 GHz methanol maser from an intermediate-mass star-forming region IRAS 22198+6336. The maser was monitored daily in 2011, 2012, and 2013. Six flares were observed with a period of 34.6 days. The variation pattern is intermittent, and the flux ratio of the flaring and the quiescent states exceeds 30. Such intermittent variation with the short period uniquely characterizes the variation of the IRAS 22198+6336 maser. At least five spectral components were identified. The spectral components varied almost synchronously, but their peak times differed by 1.8 days. These characteristics can be explained by the colliding-wind binary model.

Key words: ISM: Star forming regions — ISM: individual (IRAS 22198+6336)
— masers: methanol

1. Introduction

The 6.7 GHz methanol maser is emitted from high-mass star-forming regions (e.g., Menten 1991; Caswell et al. 1995; Minier et al. 2003; Xu et al. 2008; Breen et al. 2013). The maser is considered to trace the gas disk or outflow of young stellar objects (e.g., Minier et al. 2000; De Buizer 2003; Sugiyama et al. 2014). Since Goedhart et al. (2003, 2004) first demonstrated flux variation in this maser, several variability patterns, including periodicity,

have been recognized. The first detected periodic source was G9.62+0.20E, with a period of 246 days. To date, periodicity has been reported for 11 sources, with periods ranging from 29.5 days for G12.89+0.49 to 668 days for G196.45−1.68 (Araya et al. 2010; Goedhart et al. 2003, 2004, 2007, 2009; Szymczak et al. 2011). Some of these sources (e.g., G12.89+0.49) show continuous, sinusoidal variation, while others (e.g., G37.55+0.20) display flaring variation (with intermittently rising flux). Sugiyama et al. (2008) reported flux variation in the aperiodic source Cep A and studied the excitation mechanism and spatial distribution of its 6.7 GHz methanol maser. Fujisawa et al. (2012) discovered a bursting maser with a timescale of less than one day in G33.64−0.21, and they proposed its source as release of local magnetic energy in the gas disk. Thus, by investigating short-term flux variations of the 6.7 GHz methanol maser, we can better understand the circumstellar environments in star-forming regions.

This paper reports our observations of the 6.7 GHz methanol maser in IRAS 22198+6336. The systemic velocity of this source is -11 km s^{-1} (Tafalla et al. 1993) which is close to the velocities of the maser components. The source is located in a Cepheus–Cassiopeia molecular cloud complex (Yonekura et al. 1997), and accompanies the dark nebula Lynds 1204G (Sanchez-Monge et al. 2008) closely located to an H II region S140. From annual parallax observations, the distance of IRAS 22198+6336 was determined as $764 \pm 27 \text{ pc}$ (Hirota et al. 2008). Consequently, its luminosity and mass were derived as $450L_{\odot}$ and $7M_{\odot}$ (Hirota et al. 2008) or $370L_{\odot}$ and $5M_{\odot}$ (Sanchez-Monge et al. 2010), respectively. Given its small mass and bolometric luminosity, IRAS 22198+6336 was classified as an intermediate-mass star. Since this source is not detected by near-infrared observation, it is considered to be under formation and deeply buried in dust cloud, equivalent to a class 0 object in a low-mass star formation (Hirota et al. 2008, Sanchez-Monge et al. 2010). An outflow perpendicular to a rotating disk has been suggested for this source (Palau et al. 2011).

Our aim of this study is to observe the short-term variation and reveal the origin of the flux variation of the 6.7 GHz methanol maser. The 6.7 GHz methanol maser has not previously been reported in an intermediate-mass star-forming region and this source is the first example. Observations and results are presented in sections 2 and 3, respectively. Section 4 presents the discussion, and the paper concludes with section 5.

2. Observations

We have annually surveyed the 6.7 GHz methanol masers of approximately 200 sources between 2004 and 2007 repeatedly. Our aim is to statistically analyze the flux variation of the 6.7 GHz methanol maser (Fujisawa et al. in prep.). IRAS 22198+6336, identified as a short-term variability source, was first detected in our observations at 4.4 Jy ($V_{\text{LSR}} = -8.6 \text{ km s}^{-1}$) in 2004 (MJD of the observation day was 53226). This source was below the detection limit (3 Jy) in 2005 (MJD = 53595), was redetected at 12.1 Jy ($V_{\text{LSR}} = -18.0 \text{ km s}^{-1}$) in 2006 (MJD = 53985), and again fell below the detection limit in 2007 (MJD = 54341).

The methanol maser in IRAS 22198+6336 was monitored in 2011 and 2012 by the Yamaguchi 32-m radio telescope. The 2011 observations were performed two times every 3 days during an 83-day period from September 12 (MJD = 55816) to December 3 (MJD = 55898), yielding 41 observations (excluding missing data). Three short-time flux variations (hereafter termed flares) were detected throughout the observation. To study this variation in detail, 43 daily observations were performed during 46 days from September 27 (MJD = 56197) to November 11 (MJD = 56242) in 2012. Usual observations were done once per day as 2011. If a flare was detected, observations were increased to approximately 20 times per day throughout the flare duration. During these sub-daily observations, the maser emission of Cep A, located close to IRAS 22198+6336, was alternately monitored with the target source for flux calibration. Two sub-daily sessions were performed during the 2012 observation period. The observation system, calibration method, and accuracy of the data are reported in Fujisawa et al. (2012). The observing bandwidth, number of frequency channels, and velocity resolution were 4 MHz, 4096, and 0.044 km s^{-1} , respectively. The 1σ rms noise level was 1.4 Jy with an integration time of 14 min. In 2012, the observation bandwidth was 8 MHz, and the number of frequency channels was 8192. Other parameters were those used in the 2011 observation.

In addition, three observations were made with the Hitachi 32-m radio telescope (Yonekura et al. 2013); December 30, 2012 (MJD = 56291), January 1, 2013 (MJD = 56293), and January 11, 2013 (MJD = 56303). The observation bandwidth and number of frequency channels were 8 MHz and 8192, respectively. The system noise temperature was 30 K and the 1σ noise level was 0.3 Jy, with 5 min integration time.

3. Results

3.1. Results of 2011

Flares were detected in three sub-periods of the observation period (MJD = 55816–55823, 55847–55855, and 55886–55889). No maser spectrum with flux density exceeding 3σ was detected outside of these flare periods. A typical flare spectrum, recorded on MJD = 55819, is shown in Figure 1 (upper panel). Four spectral components, A ($V_{\text{LSR}} = -16.5 \text{ km s}^{-1}$), B (-9.1 km s^{-1}), C (-8.5 km s^{-1}), and D (-7.3 km s^{-1}), were detected at this time. Figure 2 (upper panel) shows the variation of the spectral components throughout the 2011 observation. Here, the horizontal and vertical axes specify the MJD and flux density, respectively. Although the flux density of component B is 3.2σ at MJD = 55871, this signal is disregarded since it is close to the detection limit and is absent on other days.

The flux variation of all components was intermittent, and the three flares occurred at equal intervals of approximately 35 days. During a flare, the four spectral components varied almost synchronously, although their velocities were very different (approximately 9.2 km s^{-1}). A flare lasted for approximately seven days. Lower panel of Figure 2 shows a close-up of the

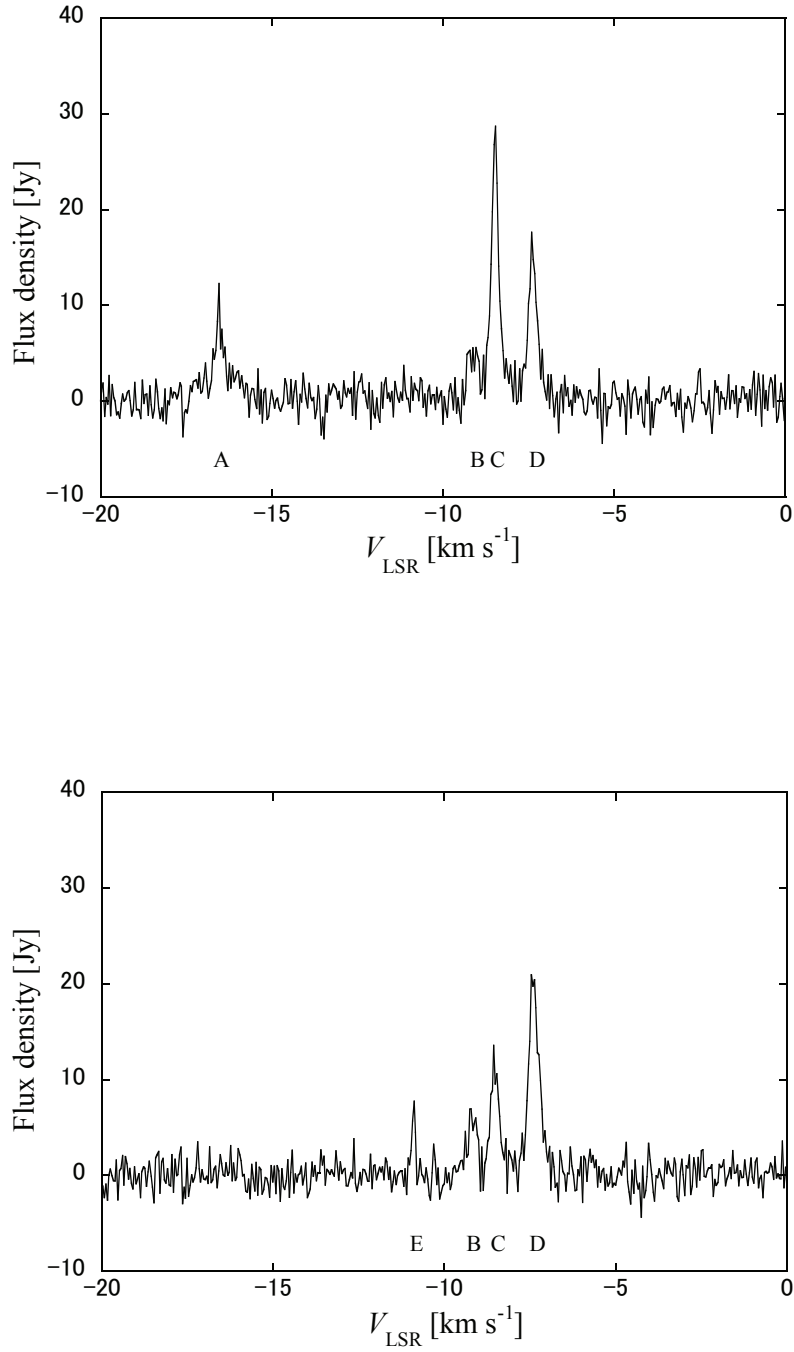


Fig. 1. Upper: Spectrum of the 6.7 GHz methanol maser of IRAS 22198+6336 observed on MJD = 55819 during the first flare in 2011. Lower: Spectrum observed in 2012 (MJD = 56235) during the second flare.

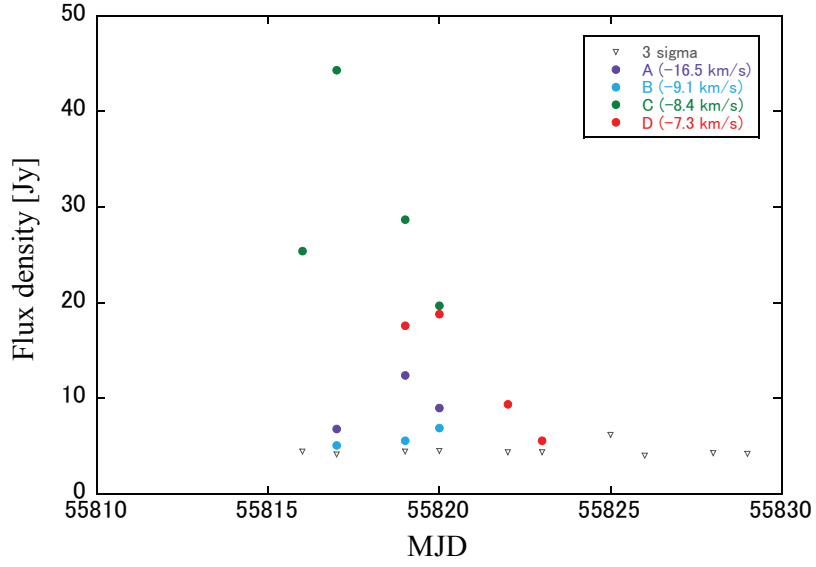
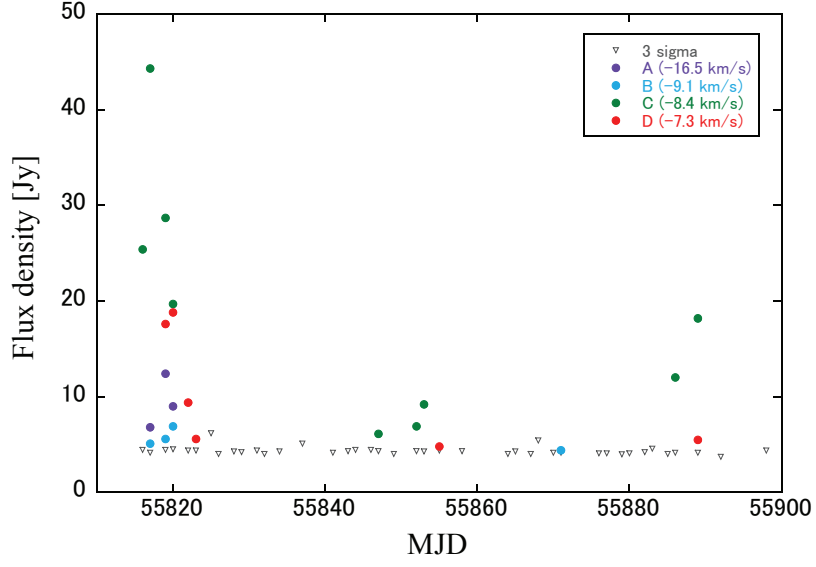


Fig. 2. Upper: Flux variation observed in 2011. Spectral components are distinguished by color: purple = A, cyan = B, green = C, and red = D. Gray triangles represent the 3σ upper limit (approximately 4 Jy). Lower: A close-up of the first flare.

first flare in 2011. Although the sparse sampling precluded a detailed light curve, the peak time of each component was clearly different; only component C is observed on MJD = 55816. The flux density of component C was its maximum but component D was not detected on the next day (MJD = 55817). Three days later (MJD = 55820), flux density of component D peaked, while the flux density of component C was down below the half of its peak. The preceding variation of C to D was also observed in the second and the third flares. Peak flux densities also differed among the flares; during the three flare periods, the flux density of component C was 44, 10, and 19 Jy.

3.2. Results of 2012

During the 2012 observation period, two flares were observed at MJD = 55198–56202 and 56231–56238. During the second flare, IRAS 22198+6336 was observed approximately 20 times per day. Spectral components B, C, and D were detected during the first flare, while B, C, D, and an additional component E (-11.0 km s^{-1}) were detected in the second flare. Component A was not detected in 2012. A spectrum taken during the second flare (MJD = 56235) is shown in Figure 1 (lower panel). The flux variation throughout the 2012 observation and close-up figures of each flare are shown in Figure 3. Again, component B was detected at 3.1σ on MJD = 56208, and was disregarded for the reasons mentioned in §3.1.

As found in the 2011 observations, two flares separated by 35 days appeared in 2012. Again, the four spectral components synchronously flared. Frequent observation in 2012 revealed the details of the flux variation. During the first flare (Figure 3 middle panel), component C showed bursting behavior, increasing rapidly from $< 4.4 \text{ Jy}$ (3σ upper-limit) to 17 Jy within one day and slowly declining over the following four days. Component D showed almost symmetrical variation in time, and the peak time of D was two days later than that of C. In the second flare, all components exhibited almost symmetrical rise and fall of flux density (Figure 3 lower panel). The peak time clearly differed among the spectral components. To quantitate these time differences, the light curves were fitted to Gaussian functions as shown in Figure 3 (lower panel) and their parameters determined. The derived parameters with their formal errors are presented in Table 1. The peak time of components B, D, and E were coincident within 0.5 days, while the peak of C differed from D by 1.8 days. The variation of C precede that of D as the same tendency was observed in the other flares in 2011 and 2012. The average FWHM of the best-fit light curves of C and D was 4 days that represent a typical time scale of the flare in IRAS 22198+6336. The relative amplitude in Table 1, a measure of variability amplitude, is defined as

$$R = \frac{S_{\max} - S_{\min}}{S_{\min}} \quad (1)$$

where S_{\max} and S_{\min} are maximum and minimum of the flux density (van der Walt et al. 2009). $S_{\min} = 4.4 \text{ Jy}$ is used here as an upper limit. The strong variability of IRAS 22198+6336 is

Table 1. Variability parameters of spectral components during the second flare in 2012.

Component	Peak flux density [Jy]	Relative amplitude	Peak time [MJD]	Time scale of variability (FWHM) [days]
B	6.5	> 0.5	56235.09 ± 0.19	6.15 ± 0.80
C	21.9	> 4.0	56233.53 ± 0.04	4.31 ± 0.09
D	19.2	> 3.4	56235.33 ± 0.02	3.72 ± 0.07
E	5.4	> 0.2	56235.61 ± 0.29	4.29 ± 1.48

remarkable since the relative amplitude of the flare exceeding 4 occurs in time scale of only 4 days. Peak flux densities differed among the flares. In the first and second flares of 2012, component C peaked at 17 and 28 Jy, respectively.

3.3. Observations with Hitachi 32-m radio telescope

Three observations were performed by the Hitachi 32-m radio telescope. No spectral component exceeding the 3σ upper limit (1.3 Jy) was detected during the first two observations (MJD = 56291 and 56293). The third observation at MJD = 56303 detected components A, B, C, and D. Component E was not detected. Figure 4 shows the spectra at MJD = 56293 and 56303. Component C yielded the highest peak flux density of 19 Jy.

3.4. The variation in 2011, 2012, and 2013

The flux variations of IRAS 22198+6336 observed in 2011, 2012, and 2013 are collectively shown in Figure 5. The dots at the bottom of the figure, indicating expected flare epochs, are spaced at 34.6-day intervals from the first flare observed at MJD = 55818 in 2011. The derivation of this interval is discussed in the next section.

4. Discussions

4.1. Periodicity

It was expected that the flare had arisen with a period of about 35 days from the observation in 2011 and 2012. The day number from the first flare of 2011 (MJD=55818) to the flare of 2013 (MJD=56303) are 485 days. This is close to 14 times of 35 days. The period of 34.6 days is derived by assuming that 485 days is exactly 14 times of the period. As shown in Fig. 5, the expected and observed flare epochs well coincide, suggesting that the flare repeats every 34.6 days. The dates of the observation performed from 2004 to 2007 were compared with the date of the flare calculated with the periodicity. The calculated MJD is 53224 and the observation MJD is 53226 with only two days difference for the 2004 observation. For the 2006 observation, the observation MJD of 53985 was just the calculated flare date. The calculated dates and the observation dates are well coincide for the 2004 and 2006 observations,

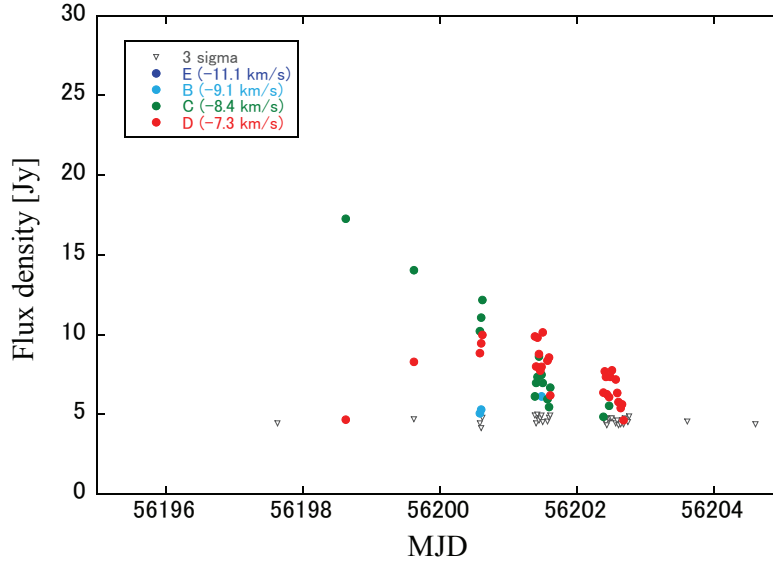
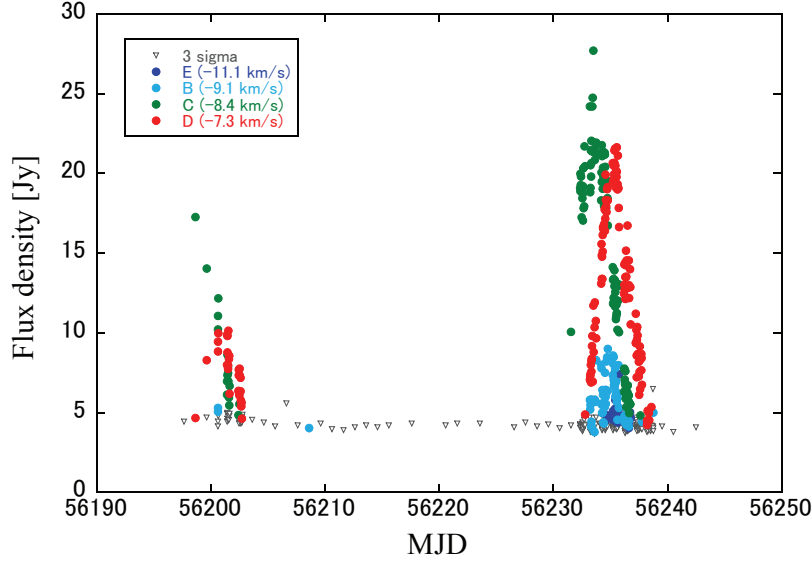


Fig. 3. Upper: flux variation observed in 2012. Spectral components are distinguished by color, as in Figure 2. Component E is represented by dark blue. Middle: detail of the first flare. Lower: detail of the second flare with best-fit curves for components C and D.

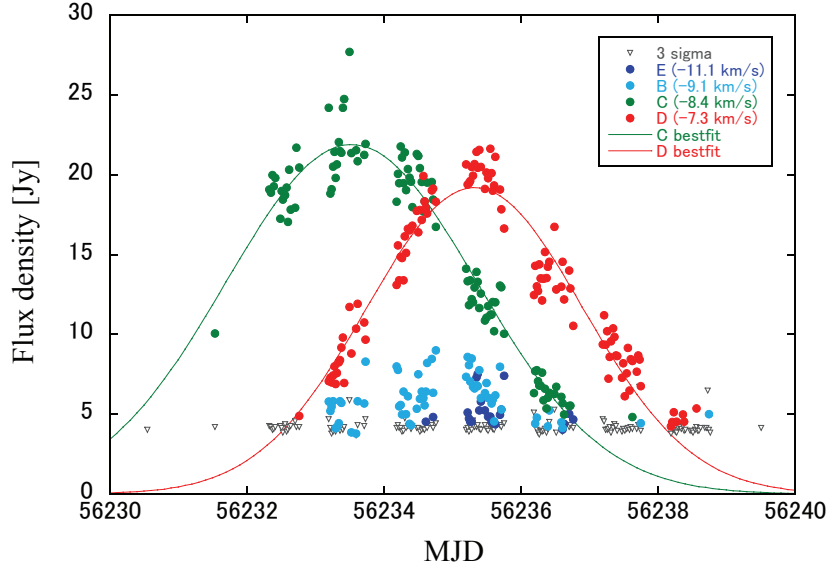


Fig. 3. cont.

and the maser emission was detected at these two observations. On the other hand, the nearest calculated date is 53605 for the observation date 53595 for the 2005 observation. For the case of 2007 observation, the nearest date is 54331 for the observation date of 54341. There are ten days difference between the calculated and observed dates for 2005 and 2007, and no maser emission was detected for these two observations. From these facts, it is suspected that the intermittent flare of 6.7 GHz methanol maser of IRAS 22198+6336 with time scale of less than 10 days occur with the period of 34.6 days, and this cycle has been kept over eight years or more than 90 cycles from 2004 to 2013.

This period of 34.6 days is the second shortest period next to the shortest one 29.5 days for G12.89+0.49 (Goedhart et al. 2009). The third shortest period is 133 days, reported for G338.93−0.06 (Goedhart et al. 2007). Thus, the period of 34.6 days for IRAS 22198+6336 is the second example of very short periodic variation sources. It is notable that all spectral components (A to E) of IRAS 22198+6336 display periodic and synchronized variation, although other periodic sources tend to exhibit periodicity in limited part of spectrum.

4.2. Variation pattern

Both continuous and intermittent variability have been recognized in the periodic variations of the 6.7 GHz methanol maser. G12.89+0.49, whose period is similar to that of IRAS 22198+6336, displayed a sinusoidal variation pattern. In contrast, IRAS 22198+6336

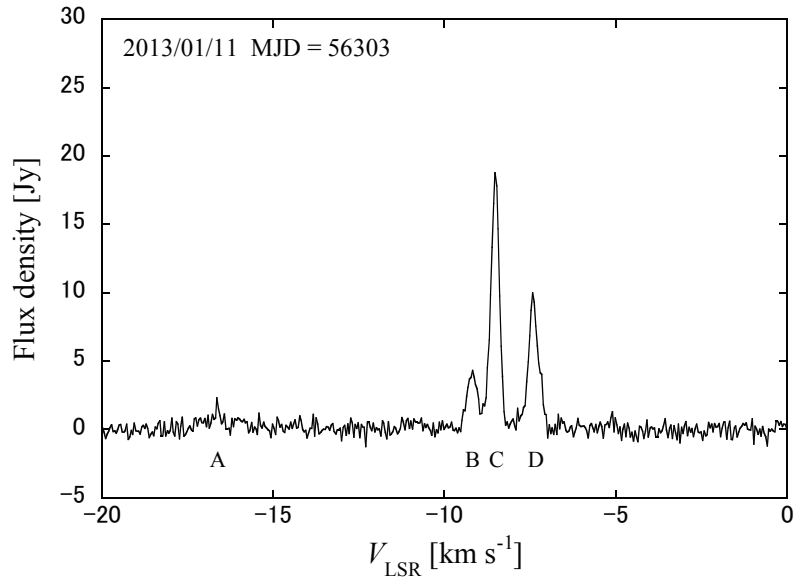
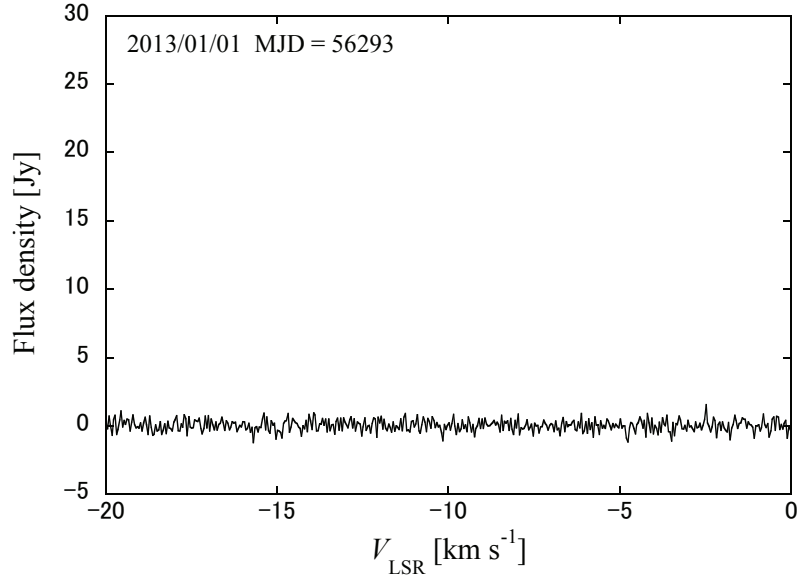


Fig. 4. Spectra of IRAS 22198+6336 observed by Hitachi 32-m. Upper: nondetection (MJD = 56293) and lower: flare (MJD = 56303).

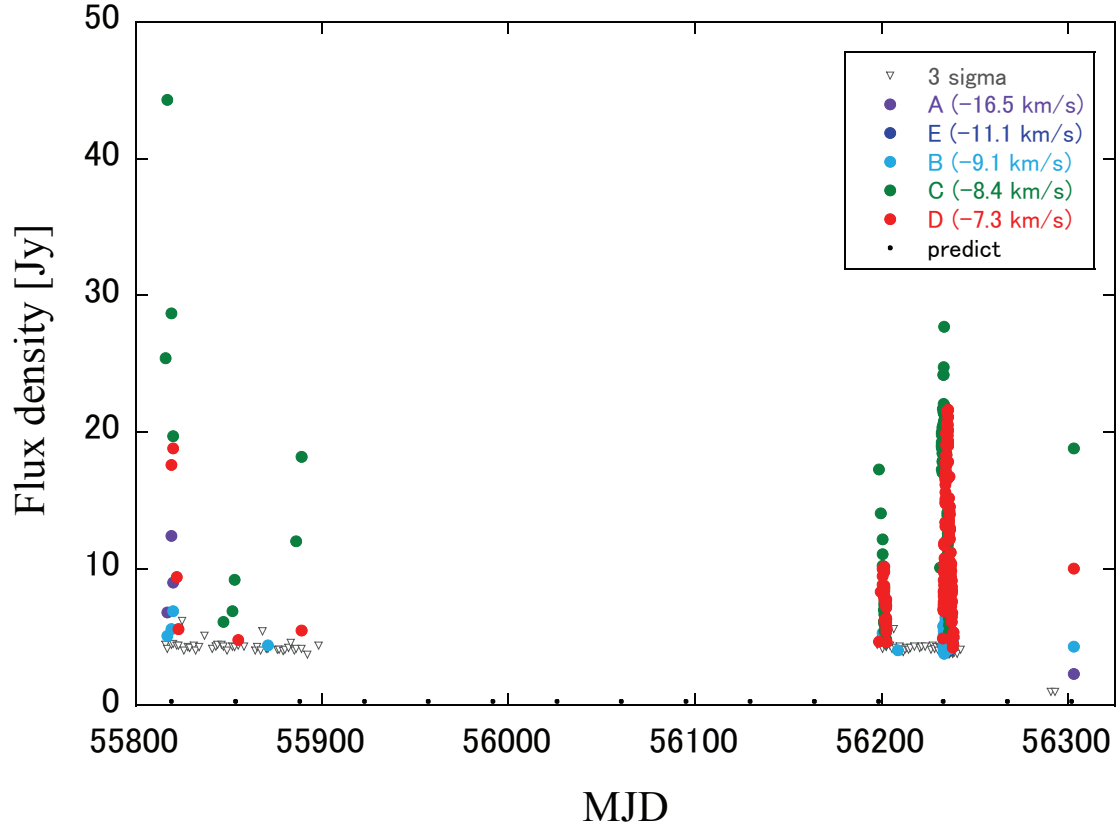


Fig. 5. Flux variation of IRAS 22193+6336 observed in 2011, 2012, and 2013. Evenly spaced dots along the MJD axis indicate dates of expected flares.

varied intermittently. According to the Hitachi 32-m observations, the flux density during the quiescent state is less than or equal to 1.3 Jy. During the first flare of 2011, the flux density exceeded 40 Jy. The relative amplitude of the peak flux density to the quiescent flux density exceeds 30. Similar intermittent flux variations have been reported for G22.356+0.066 (Szymczak et al. 2011), G328.24−0.55 (Goedhart et al. 2007), G37.55+0.20 (Araya et al. 2010), and G9.62+0.20E (Goedhart et al. 2003) although the relative amplitude of these sources are smaller, i.e., 5 for G22.356+0.066, 1 for G328.24−0.55, 10 for G37.55+0.20, and 0.2 for G9.62+0.20E, respectively. Table 2 compares the variability of IRAS 22198+6336 with that of 11 known periodically variable sources. Listed are the period, variation pattern (intermittent or sinusoidal), variation range of flux density, and relative amplitude. The variation patterns are visually judged from the light curve, and the variation ranges are read from the figures in the reference papers. Among the recorded sources, IRAS 22198+6336 exhibits the short variation period and the intermittent variation pattern, with the highest relative amplitude exceeding 30. Such intermittent variation with the short period uniquely characterizes the variation of the IRAS 22198+6336 maser.

We note that the short-period variation of less than 30 days would be undetectable if such sources were observed once per month or less frequently. This means a possibility that there are other short-period sources like IRAS 22198+6336 which are not yet recognized as periodic variable sources. Moreover, it is only about 20 % of the period that IRAS 22198+6336 exhibits the detectable maser emission. Therefore the detection probability of IRAS 22198+6336 is only 20 % for single observation. There might be strong flaring sources like IRAS 22198+6336 not yet discovered by surveys done so far. Repeating survey observation would be required for discovery of strong variable sources similar to IRAS 22198+6336.

The peak times of different spectral components are known to vary in some periodic variable sources as observed in IRAS 22198+6336 (e.g., G12.89+0.49; Goedhart et al. 2009). This peak time difference could be explained as follows: the maser spots of each component are distributed around an exciting source and all spectral components intrinsically vary together following the variation of the exciting source. Then the time lag would be caused by the different distances between the maser spots and the observer. Based on this model, Szymczak et al. (2011) constructed a three-dimensional distribution of maser spots of G22.357+0.066. In IRAS 22198+6336 observations, the peak time of spectral components C and D differed by 1.8 days, which corresponds to a separation distance of 310 AU to the line-of-sight. This distance could be compared with the spatial distribution of the 6.7 GHz methanol maser emission region of IRAS 22198+6336 derived from the luminosity of the source. Given that the luminosity and the exciting dust temperature of the maser region is $450L_{\odot}$ (Hirota et al. 2008) and 100 K (Cragg et al. 2005), respectively, the distribution of the maser emission region is derived as 330 AU. This is close to the separation distance of 310 AU derived from the peak time lag. Future VLBI observation is expected to reveal the spatial distribution of the maser spots of

Table 2. Comparison of variation properties among periodic 6.7 GHz methanol maser sources.

Name	Period [day]	Variation pattern	Variation range [Jy]	Relative Amplitude	Reference
G12.89+0.49	29.5	sinusoidal	5–20	3	1
IRAS22198+6336	34.6	intermittent	<1.3–44	> 30	this paper
G338.93–0.06	133	sinusoidal	20–50	1.5	2
G22.357+0.066	179	intermittent	1–6	5	3
G339.62–0.12	201	sinusoidal	30–100	2	2
G328.24–0.55	220	intermittent	200–400	1	2
G37.55+0.20	237	intermittent	0.5–5	10	4
G9.62+0.20E	246	intermittent	4500–5500	0.2	5
G12.68–0.18	307	sinusoidal	40–100	1.5	6
G188.95+0.89	404	sinusoidal	500–600	0.2	2
G331.13–0.24	504	sinusoidal	1–20	20	2
G196.45–1.68	668	sinusoidal	20–40	1	6

References — 1: Goedhart et al. (2009), 2: Goedhart et al. (2007), 3: Szymczak et al.

(2011), 4: Araya et al. (2010), 5: Goedhart et al. (2003), and 6: Goedhart et al. (2004).

this source.

4.3. Flaring mechanism

Several mechanisms responsible for maser variability have been proposed. The mechanisms proposed are, for example, interstellar scintillation (Clegg & Cordes 1991), maser overlap (Shimoikura et al. 2005), and release of local magnetic energy (Fujisawa et al. 2012). However, none of these models can explain the characteristics of the varying 6.7 GHz methanol maser of IRAS 22198+6336, such as its periodicity, synchronization and time lag of spectral components, and flaring variation pattern. To explain these variability characteristics, the model must incorporate a periodic and intermittent luminosity variation of the exciting source, which will be reflected in the maser behavior.

According to theory, high-mass protostars that accrete gas with high accretion rate larger than $10^{-3}M_{\odot}\text{yr}^{-1}$ should pulsate, thereby periodically altering their radius, temperature, and luminosity (Inayoshi et al. 2013). Such pulsation should also yield periodic variation of the excitation state and flux density. However, the expected variation is sinusoidal, and this model cannot easily explain the short-term flare. In addition, given the luminosity ($450L_{\odot}$) of IRAS 22198+6336, the expected period is approximately one day; alternatively, the luminosity expected from the period (34.6 days) is $1.4 \times 10^4 L_{\odot}$. Both quantities differ from their observed values.

van der Walt et al. (2009) proposed the colliding-wind binary (CWB) model, which incorporates a binary system with large eccentricity for interpreting the periodic flare observed

in G9.62+0.20E. When a companion star passes the periastron, the shock induces ionization photons and heat the surrounding gas and dust. The observed maser variability would then be caused by the enhancement of the seed photon from the ionized gas. The light curve of the periodic flare of G9.62+0.20E showed a rapid rise and slow decay, and the time scale of decay was about 100 days. They discussed that the time scale of 100 days can be explained by the characteristic recombination time of an HII region which is the origin of the seed photon of the maser emission. The CWB model qualitatively explains the observed characteristics of IRAS 22198+6336, such as its periodicity and flaring variability. Assuming that a companion star of mass $1M_{\odot}$ orbits the $7M_{\odot}$ primary star in 34.6 days, the semi-major axis of the binary is 0.41 AU, which is not unexceptional in a binary system.

The periodic variability of G9.62+0.20E were observed at specific spectral components while the other components did not show the periodicity. This could be interpreted as that only the maser clouds locating near side of the HII region would be strengthened by the seed photon enhancement and show periodic variability. Unlike the case of G9.62+0.20E, all the spectral components with the 9.2 km s^{-1} velocity difference flared synchronously in IRAS 22198+6336. Moreover, there was a time lag of 1.8 days between spectral components. If the maser emission is enhanced by the seed photons of the HII region strengthened by the shock induced by the periastron passage, all the maser emission vary without time lag. In addition, IRAS 22198+6336 is relatively low luminosity with intermediate-mass exciting star, there would be no (Ultra-Compact) HII region around the star.

Alternatively, the enhancement of the excitation photon by heated dust would explain above characteristics of the periodic flare of IRAS 22198+6336. The cooling time of optically thick dust radiation is about 1.2 days (van der Walt et al. 2009) which is shorter than the time scale of the flare. The dust temperature would follow the variation of the strength of heating radiation without large delay. During the first flare of component D and the second flare of C and D (probably B and E too) in 2012, the light-curve displayed a symmetry in time, in contrast to that the other sources of intermittent variation tend to show rapid rise and slow decay (G9.62+0.20E, van der Walt et al. 2009; G22.357+0.066, Szymczak et al. 2011). Since the interaction of a binary star would arise symmetrically in time to the periastron, the strength of heating radiation, the dust temperature, and the enhancement of maser excitation would occur symmetrically in time, consequently the time symmetry of the light-curve of the flare would be explained. The flare last only short time and the maser is undetectable at 80% of the period suggesting the large eccentricity of a binary star (van der Walt et al. 2009).

4.4. *Water and methanol maser*

Finally we would like to point out the coincidence of the methanol and water masers in IRAS 22198+6336. The 6.7 GHz methanol maser spectrum of IRAS 22198+6336 shows a good correspondence with the 22 GHz water maser spectrum (Hirota et al. 2008). The spec-

tral components of the water maser of the almost same velocity exist for the methanol maser components A (-16.5 km s^{-1}), B (-9.1 km s^{-1}), and C (-8.4 km s^{-1}). Moreover, the spatial distribution expected from the time lag of the methanol maser variation is 310 AU, corresponding to 400 mas in the sky, which is in good agreement with the size of distribution of the water maser (Hirota et al. 2008). According to these facts, the emission region of the methanol maser of IRAS 22198+6336 may be the same or very close to the emission region of the water maser. Bartkiewicz et al. (2011) reported that there are sources similar to IRAS22198+6336 showing the close velocity distributions of water and methanol masers. However, it is revealed by VLBI observations that water maser shows different spatial distributions to that of methanol maser in some sources (e.g., Sugiyama et al. 2008, 2011). The excitation mechanism of the water maser is considered to be collisional in contrast to the radiation excitation working for the 6.7 GHz methanol maser. Generally, the water maser has arisen in the region at which outflow of YSO collides with the surrounding materials. Although the water maser observed by IRAS 22198+6336 shows flux variability, flare or periodicity like the 6.7 GHz methanol maser have not been reported. Therefore, coincidence of the spectrum and the spatial scale may be a coincidence by chance. Bartkiewicz et al. (2011) noted that water and methanol masers probe different part of the environment of star forming regions.

Nonetheless, if the distribution of methanol and water maser is actually spatially close, the cause may be explained as follows. Once the outflow of YSO collides with the surrounding materials, the gas is compressed by the shock and its density and temperature increase, consequently the water maser is excited and emitted. Simultaneously, the density of the region is high enough for emitting the methanol maser by radiation excitation by a central star. This model may also be able to explain that there is a case which methanol maser appears from the shock region produced by outflow as pointed out by De Buizer (2003). This model would be verifiable by the spatial distribution and proper motion observations of methanol and water masers by VLBI monitoring in future.

5. Conclusions

We report periodic flaring of the 6.7 GHz methanol maser in an intermediate-mass star forming region IRAS 22198+6336. IRAS 22198+6336 is the first intermediate-mass source detected by the 6.7 GHz methanol maser. Six flares were detected during observations undertaken in 2011, 2012, and 2013. The peak flux density exceeded 40 Jy, but was below the detection limit of 1.3 Jy in the quiescent phase. The flare periodically erupted every 34.6 days. The time scale of a single flare was as short as 4 days, and rapid flux variation was observed. Including IRAS 22198+6336, periodic variability of the 6.7 GHz methanol maser has been reported in 12 sources to date. The periodic variability of IRAS 22198+6336 is uniquely characterized by its short period and its flaring nature, and is reasonably explained by the CWB model.

The authors thank Mr. Hiramoto for his assistance to the data analysis, National Astronomical Observatory of Japan, KDDI Corporation for supporting the Yamaguchi 32-m radio telescope. This work was financially supported in part by Grant-in-Aid for Scientific Research (KAKENHI) from the Japan Society for the Promotion of Science (JSPS), No. 24340034.

References

- Araya, E. D., Hofner, P., Goss, W. M., Kurtz, S., Richards, A. M. S., Linz, H., Olmi, L., & Sewilo, M. 2010, *ApJL*, 717, L133
- Bartkiewicz, A., Szymczak, M., van Langevelde, H. J., Richards, A. M. S., & Pihlström, Y. M. 2009, *A&A*, 502, 155
- Breen, S. L., Ellingsen, S. P., Contreras, Y., Green, J. A., Caswell, J. L., Stevens, J. B., Dawson, J. R., & Voronkov, M. A. 2013, *MNRAS*, 435, 524
- Caswell, J. L., Vaile, R. A., Ellingsen, S. P., Whiteoak, J. B., & Norris, R. P. 1995, *MNRAS*, 272, 96
- Clegg, A. W., & Cordes, J. M. 1991, *ApJ*, 374, 150
- Cragg, D. M., Sobolev, A. M., & Godfrey, P. D. 2005, *MNRAS*, 360, 533
- De Buizer, J. M. 2003, *MNRAS*, 341, 277
- Fujisawa, K., Sugiyama, K., Aoki, N., Hirota, T., Mochizuki, N., Doi, A., Honma, M., Kobayashi, H., Kawaguchi, N., Ogawa, H., Omodaka, T., & Yonekura, Y. 2012, *PASJ*, 64, 17
- Goedhart, S., Gaylard, M. J., & van der Walt, D. J. 2003, *MNRAS*, 339, 33
- Goedhart, S., Gaylard, M. J., & van der Walt, D. J. 2004, *MNRAS*, 355, 553
- Goedhart, S., Gaylard, M. J., & van der Walt, D. J. 2007, *Astrophysical Masers and their Environments*, Proceedings of the International Astronomical Union, IAU Symposium, Volume 242, p. 97-101
- Goedhart, S., Langa, M. C., Gaylard, M. J., & van der Walt, D. J. 2009, *MNRAS*, 398, 995
- Hirota, T., Ando, K., Bushimata, T., Choi, Y. K., Honma, M., Imai, H., Iwadate, K., Jike, T., Kameno, S., Kameya, O. et al. 2008, *PASJ*, 60, 961
- Inayoshi, K., Sugiyama, K., Hosokawa, T., Motogi, K., & Tanaka, K. E. I. 2013, *ApJ*, 769, 20
- Menten, K. M. 1991, *ApJ*, 380, 75
- Minier, V., Booth, R. S., & Conway, J. E. 2000, *A&A*, 362, 1093
- Minier, V., Ellingsen, S. P., Norris, R. P., & Booth, R. S. 2003, *A&A*, 403, 1095
- Palau, A., Fuente, A., Girart, J. M., Fontani, F., Boissier, J., Pietu, V., Sanchez-Monge, A., Busquet, G., Estalella, R., Zapata, L. A., Zhang, Q., Neri, R., Ho, P. T. P., Alonso-Albi, T., & Audard, M. 2011, *ApJ*, 743, 32
- Sanchez-Monge, A., Palau, A., Estalella, R., Beltran, M. T., & Girart, J. M. 2008, *A&A*, 485, 497
- Sanchez-Monge, A., Palau, A., Estalella, R., Kurtz, S., Zhang, Q., Di Francesco, J., & Shepherd, D. 2010, *ApJ*, 721, 107
- Shimoikura, T., Kobayashi, H., Omodaka, T., Diamond, P. J., Matveyenko, L. I., & Fujisawa, K. 2005, *ApJ*, 634, 459

- Sugiyama, K., Fujisawa, K., Doi, A., Honma, M., Isono, Y., Kobayashi, H., Mochizuki, N., & Murata, Y. 2008, PASJ, 60, 1001
- Sugiyama, K., Fujisawa, K., Doi, A., Honma, M., Isono, Y., Kobayashi, H., Mochizuki, N., Murata, Y., Sawada-Satoh, S., & Wajima, K. 2011, PASJ, 63, 53
- Sugiyama, K., Fujisawa, K., Doi, A., Honma, M., Kobayashi, H., Murata, Y., Motogi, K., Niinuma, K., Ogawa, H., Wajima, K., Sawada-Satoh, S., & Ellingsen, S. P. 2014, A&A, 562, 82
- Szymczak, M., Wolak, P., Bartkiewicz, A., & van Langevelde, H. J. 2011, A&A, 531, L3
- Tafalla, M., Bachiller, R., & Martin-Pintado, J. 1993, ApJ, 403, 175
- van der Walt, D. J., Goedhart, S., & Gaylard, M. J. 2009, MNRAS, 398, 961
- Xu, Y., Li, J. J., Hachisuka, K., et al. 2008, A&A, 485, 729
- Yonekura, Y., Dobashi, K., Mizuno, A., Ogawa, H., & Fukui, Y. 1997, ApJS, 110, 21
- Yonekura, Y., Saito, Y., Saito, T., et al. 2013, ASP Conf. Ser. 476: New Trends in Radio Astronomy in the ALMA Era: The 30th Anniversary of Nobeyama Radio Observatory (eds. R. Kawabe, N. Kuno, S. Yamamoto), 415

